

OPTIMALLY SWIMMING STOKESIAN ROBOTS

FRANÇOIS ALOUGES*, ANTONIO DESIMONE †, LUCA HELTAI‡, ALINE LEFEBVRE-LEPOT§, AND BENOÎT MERLET¶

Abstract. We study self-propelled stokesian robots composed of assemblies of balls, in dimensions 2 and 3, and prove that they are able to control their position and orientation. This is a result of *controllability*, and its proof relies on applying Chow's theorem in an analytic framework, similar to what has been done in [3] for an axisymmetric system swimming along the axis of symmetry. We generalize the analyticity result given in [3] to the situation where the swimmers can move either in a plane or in three-dimensional space, hence experiencing also rotations. We then focus our attention on energetically optimal strokes, which we are able to compute numerically. Some examples of computed optimal strokes are discussed in detail.

1. Introduction. Self-propulsion at low Reynolds number is a problem of considerable biological and biomedical relevance which has also great appeal from the point of view of fundamental science. Starting from the pioneering work by Taylor [32] and Lighthill [24], it has received a lot of attention in recent years (see the encyclopedia article [4] for an elementary introduction and the review paper [22] for a comprehensive list of references).

Both relevance for applications and theoretical interest stem from the fact that one considers swimmers of small size. The Reynolds number $Re = LV/\nu$ gives an estimate for the relative importance of inertial to viscous forces for an object of size L moving at speed V through a newtonian fluid with kinematic viscosity ν . Since in applications V rarely exceeds a few body lengths per second, if one considers swimming in a given medium, say, water, then Re is entirely controlled by L . At small L , inertial forces are negligible and, in order to move, micro-swimmers can only exploit the viscous resistance of the surrounding fluid. The subtle consequences of this fact (which are rather paradoxical when compared to the intuition we can gain from our own swimming experience) are discussed in [30]. For example, the motion of microswimmers is geometric: the trajectory of a low Re swimmer is entirely determined by the sequence of shapes that the swimmer assumes. Doubling the rate of shape changes simply doubles the speed at which the same trajectory is traversed. As observed in [31], this suggests that there must be a natural, attractive mathematical framework for this problem (which the authors, indeed, unveil). On the other hand, bacteria and unicellular organisms *are* of micron size, while artificial robots to be used non-invasively inside human bodies for medical purposes *must* be small. Discovering the secrets of biological micro-swimmers and controlling engineered micro-robots requires a quantitative understanding of low Re self-propulsion.

The basic problem of swimming is easy to state: given a (periodic) time history of shapes of a swimmer (a sequence of strokes), determine the corresponding time

*CMAP UMR 7641, École Polytechnique CNRS, Route de Saclay, 91128 Palaiseau Cedex - France (francois.alouges@polytechnique.edu)

†SISSA, International School of Advanced Studies, Via Bonomea 265, 34136 Trieste - Italy (desimone@sissa.it)

‡SISSA, International School of Advanced Studies, Via Bonomea 265, 34136 Trieste - Italy (luca.heltai@sissa.it)

§CMAP UMR 7641, École Polytechnique CNRS, Route de Saclay, 91128 Palaiseau Cedex - France (aline.lefebvre@polytechnique.edu)

¶CMAP UMR 7641, École Polytechnique CNRS, Route de Saclay, 91128 Palaiseau Cedex - France (benoit.merlet@polytechnique.edu)

history of positions and orientations in space. A natural, related question is the following: starting from a given position and orientation, can the swimmer achieve any prescribed position and orientation by performing a suitable sequence of strokes? This is a question of *controllability*. The peculiarity of low Re swimming is that, since inertia is negligible, reciprocal shape changes lead to no net motion, so the question of controllability may become non trivial for swimmers that have only a few degrees of freedom at their disposal to vary their shape. The well established scallop theorem [30] is precisely a result of non-controllability.

Once controllability is known, i.e., it is shown that it is possible to go from A to B, one can ask the question of how to go from A to B at minimal energetic cost. This is a question of *optimal control*.

In spite of the clear connections between low Re self-propulsion and control theory, this viewpoint has started to emerge only recently, and mostly in the mathematical literature. Examples are [21], and the more recent contributions [10], [11], [20] and [26]. The papers [2], [3], [4] study in detail both controllability and optimal control for axisymmetric swimmers whose varying shapes are described by few (in particular, two) scalar parameters.

In this paper we analyze the problem of low Reynolds number swimming from the point of view of geometric control theory, and focus on a special class of model systems: those obtained as assemblies of a small number of balls. Model systems of this type have played an important role in clarifying the subtleties of low Re self-propulsion [27], [6], [13]. These systems offer an interesting balance between complexity of the analysis and richness of observable behavior.

While constructing such artificial swimmers may indeed be possible, their practical uses are at present unclear. However, the analysis of their swimming patterns may prove a very useful tool both in the design of robotic microswimmers [14], and in understanding the motion of biological swimmers. As an example, the social motility patterns exhibited by Myxobacteria (see, e.g., [18]) are strikingly similar to the ones described in this paper. As part of their life cycle, individual cells become linked together and move collectively on surfaces. The links between adjacent cells are guaranteed by pili which individual cells can project and retract. The fact that collective motion rests upon control of the relative positions of individuals seems fully established. Our study may shed light on the many details that are at present unclear.

Proving controllability and providing optimal control strategies for realistic swimmers, either biological or artificial, is rather difficult. The use of assembly of balls as a model swimmer relies on the idea that one can use collections of spheres to model the hydrodynamic characteristics of real swimmers, replacing their actual swimming apparatus (which can be indeed very complex to describe, simulate and approximate) with a finite collection of spheres having comparable hydrodynamic resistance. Very recent progress towards the analysis of low Re more general swimmers propelling through shape changes can be found in [12], [25].

Our approach is similar in spirit to the one in [2], [3], [4], but we extend it to non-axisymmetric systems such as three spheres moving in a plane, and systems of four spheres moving in three dimensional space. The motion of these systems is described by both positional and orientational variables, leading to a much richer geometric structure of the state space. The study of such systems requires substantial extensions of the mathematical and numerical methods introduced in [3].

For all the model swimmers described above, controllability is proved by using two main ingredients. The first is Chow's theorem, leading to local controllability in

a neighborhood of a point X in state space. We verify the full rank (5.2) hypothesis of this theorem by showing that the vector fields of the coefficients of the governing ODEs (a linear control system without drift) and their first order Lie brackets span the whole tangent space to the state space at X . The second is the analyticity of the coefficients, and the fact that our shape space is always connected. This allows us to pass from local to global controllability generalizing a result that has been proved in [3] for the special axisymmetric case. In the same paper [3], Chow's theorem was also used to prove local controllability. In this simpler axisymmetric case, however, position is described only by one scalar parameter (the position p of one distinguished point along the axis of symmetry). The non-degeneracy condition reduces then to the non-vanishing of a single scalar quantity, namely, the curl of the vector field \mathbf{V} , governing the rate of change of position as a consequence of shape changes at rates ξ_i according to $\dot{p} = \mathbf{V}_1(\xi)\xi_1 + \mathbf{V}_2(\xi)\xi_2$. In the richer context of this paper, which involves also rotational degrees of freedom of the swimmers, proving controllability requires an explicit computation of all the first order Lie Brackets. In fact, all the systems we analyze here satisfy the condition

$$M + M(M - 1)/2 = d$$

where M is the number of controls (rate of change of shape variables) and d is the dimension of the state space (position, orientation, and shape). This is the necessary condition that first order Lie brackets alone suffice to show that the Lie algebra of the coefficients has full rank, so that controllability follows.

For controllable systems, it makes sense to ask how to achieve the desired target (position and orientation) at minimal energy cost. We present a method to address this optimal control question numerically, and we then examine in detail several optimal strokes for a concrete model swimmer (three balls swimming in a plane with a prescribed lateral displacement). Depending on whether the final orientation is also prescribed, and whether the initial shape is prescribed as well or rather one treats it as a parameter to be optimized, we obtain dramatically different answers. Their variety illustrates the surprisingly richness of behavior of low Re swimmers.

The rest of the paper is organized as follows. In Section 2, we describe the various model swimmers to which our analytical and numerical tools are later applied. The first is the Najafi-Golestanian's swimmer [27], already treated in [3], while the two others are non-trivial generalizations. Section 3 presents some results on Stokes flows and in Section 4 we show that swimming is indeed an affine control problem without drift. In Section 5, we prove the effective swimming capability of our model swimmers. In Sections 6 and 7 we state the optimal control problem and a numerical strategy for its solution. Examples of optimal strokes for three balls swimming in a plane are discussed in detail in Section 8.

2. The swimmers. We will focus our attention on some special swimmers. Namely, we assume that the swimmer is composed of N non-intersecting balls $(B_i)_{1 \leq i \leq N} \subset \mathbb{R}^3$ centered at $(\mathbf{x}_i)_{1 \leq i \leq N}$, and we restrict ourselves to configurations which can be described by two sets of variables:

- the *shape variables*, denoted by $\xi \in \mathcal{S}$, where \mathcal{S} is an open connected subset of \mathbf{R}^M , from which relative distances $(\mathbf{x}_{ij})_{1 \leq i, j \leq N}$ between the balls $(B_i)_{1 \leq i \leq N}$ are obtained. In the examples treated in this paper, the balls are assumed to move only along fixed directions which make fixed angles one to another. This reflects a situation where the balls are linked together by thin jacks that are able to elongate. The viscous resistance associated with these jacks



FIG. 2.1. *Three Sphere Swimmer (3S)*

is, however, neglected, and the fluid is thus assumed to fill the whole set $\mathbb{R}^3 \setminus \bigcup_{i=1}^N B_i$.

- the *position variables*, denoted by $p \in \mathcal{P}$, which describe the global position and orientation in space of the swimmer. In our examples, the set \mathcal{P} is typically a manifold of dimension less than or equal to six. The six-dimensional case is given by $p \in \mathcal{P} = \mathbf{R}^3 \times \text{SO}(3)$ and p consists of a translation and a rotation in the three-dimensional space.

We also assume that the orientation of the balls $(B_i)_{1 \leq i \leq N}$ and the distances $(\mathbf{x}_{ij})_{1 \leq i, j \leq N}$ depend analytically on (ξ, p) , therefore the state of the system is analytically and uniquely determined by the variables (ξ, p) , so that there exist N (analytic) functions

$$\mathbf{X}_i : \mathcal{S} \times \mathcal{P} \times \partial B \longrightarrow \mathbf{R}^3$$

which give the position of the current point of the i -th sphere of the swimmer in the state (ξ, p) in $\mathcal{S} \times \mathcal{P}$. The non-slip boundary condition on ∂B_i imposes that the velocity of the fluid is given by

$$\mathbf{v}_i(\xi, p, \mathbf{r}) = \frac{d}{dt} \mathbf{X}_i(\xi, p, \mathbf{r}) = (\dot{\xi} \cdot \nabla_{\xi}) \mathbf{X}_i(\xi, p, \mathbf{r}) + (\dot{p} \cdot \nabla_p) \mathbf{X}_i(\xi, p, \mathbf{r}). \quad (2.1)$$

2.1. The three sphere swimmer of Najafi and Golestanian (3S). This swimmer, initially proposed in [27] has been studied thoroughly in [3] and [5]. It is composed of 3 spheres of radius $a > 0$ aligned along the x -axis, as depicted in Fig. 2.1.

We call $\xi = (\xi_1, \xi_2)$ the length of the arms, and p the position of the central sphere which leads us, in order to avoid overlap of the spheres, to consider the shape set $\mathcal{S} = (2a, +\infty)^2$ and the position set $\mathcal{P} = \mathbf{R}$. Indeed, due to axial symmetry, this swimmer may only move along the x -axis. Using $\mathbf{e}_1 = (1, 0, 0)^T$, we can write

$$\mathbf{x}_1(\xi, p) = (p - \xi_1) \mathbf{e}_1, \mathbf{x}_2(\xi, p) = p \mathbf{e}_1, \mathbf{x}_3(\xi, p) = (p + \xi_2) \mathbf{e}_1,$$

and

$$\mathbf{X}_i(\xi, p, \mathbf{r}) = \mathbf{x}_i(\xi, p) + \mathbf{r}, \quad \forall i \in \{1, 2, 3\}, \forall \mathbf{r} \in \partial B.$$

2.2. The three sphere swimmer moving in a plane (3SP). A variant of the Najafi-Golestanian's swimmer, called "*Purcell's rotator*", was presented in [13], where the axis along which the three spheres are constrained to move, is bent to form a circle with fixed radius. The resulting swimmer is one where the three spheres always keep a fixed distance from the center of the swimmer, and may only vary their location on the circle, remaining on the same plane.

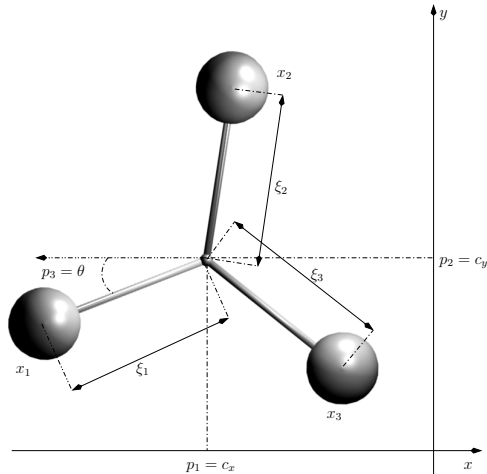


FIG. 2.2. *The three-sphere planar swimmer (3SP)*

As observed in [13], this variation allows one to control rotations around the axis perpendicular to the circle and passing through the center of the swimmer (hence the name “rotator”), and introduces as well a small drift in the system, which displaces horizontally on the plane containing the circle.

That swimmer does not change the number of controls (two) with respect to the Najafi Golestanian’s swimmer, however a periodic shape change induces both a rotation *and* a translation of the swimmer (that is, the dimension d of the state space is equal to $5 \neq M + M(M - 1)/2 = 3$). Seen from the perspective of control theory, this implies that not only first order Lie brackets are used to change the positional variables but also higher order ones, with smaller and smaller effectiveness as the order of the used Lie brackets increases (see Section 5).

A complementary version of Purcell’s rotator, with one additional control variable, has been proposed and studied in [23]. It is composed of three balls B_1, B_2, B_3 of equal radii $a > 0$. The three balls can move along three horizontal axes that mutually meet at \mathbf{c} with angle $\frac{2\pi}{3}$ (see Fig. 2.2). The balls do not rotate around their axes so that the shape of the swimmer is characterized by the three lengths ξ_1, ξ_2, ξ_3 of its arms, measured from the origin to the center of each ball. However, the swimmer may freely rotate around \mathbf{c} in the horizontal plane.

Consider a reference equilateral triangle (S_1, S_2, S_3) with center $O \in \mathbf{R}^3$ in the horizontal plane (O, x, y) such that $\text{dist}(O, S_i) = 1$ and define $\mathbf{t}_i = \vec{OS}_i$. Position and orientation in the horizontal plane are described by the coordinates of the center $\mathbf{c} \in \mathbf{R}^3$ (but \mathbf{c} stays confined to the horizontal plane) and the horizontal angle θ that one arm, say arm number 1, makes with a fixed direction, say (O, x) , in such a way that $d = 3$. Therefore, we place the center of the ball B_i at $\mathbf{x}_i = \mathbf{c} + \xi_i \mathcal{R}_\theta \mathbf{t}_i$ with $\xi_i > 0$ for $i = 1, 2, 3$, where \mathcal{R}_θ stands for the horizontal rotation of angle θ given for instance by the matrix:

$$\mathcal{R}_\theta = \begin{pmatrix} \cos(\theta) & -\sin(\theta) & 0 \\ \sin(\theta) & \cos(\theta) & 0 \\ 0 & 0 & 1 \end{pmatrix}.$$

The swimmer is then fully described by the parameters $X = (\xi, \mathbf{c}, \theta) \in \mathcal{S} \times \mathcal{P}$,

where $\mathcal{S} := (\frac{2a}{\sqrt{3}}, +\infty)^3$, the lower bound being chosen in order to avoid overlaps of the balls, $\mathcal{P} = \mathbf{R}^2 \times \mathbf{R}$, and the functions \mathbf{X}_i are now defined as

$$\mathbf{X}_i(\xi, \mathbf{c}, \alpha, \mathbf{r}) = \mathbf{c} + \mathcal{R}_\theta(\xi_i \mathbf{t}_i + \mathbf{r}) \quad \forall i \in \{1, 2, 3\}.$$

Notice that the functions \mathbf{X}_i are still analytic in $(\xi, \mathbf{c}, \theta)$, and we use them to compute the instantaneous velocity on the sphere B_i

$$\mathbf{v}_i = \frac{\partial \mathbf{X}_i}{\partial t}(\xi, \mathbf{c}, \theta, r) = \dot{\mathbf{c}} + \dot{\theta} \mathbf{e}_3 \times (\xi_i \mathbf{t}_i + \mathbf{r}) + \mathcal{R}_\theta \mathbf{t}_i \dot{\xi}_i,$$

where \mathbf{e}_3 is the vertical unit vector. Eventually, due to the symmetries of the system, the swimmer stays in the horizontal plane.

2.3. The four sphere swimmer moving in space (4S). We now turn to the more difficult situation of a swimmer able to move in the whole three dimensional space and rotate in any direction. In this case, we fix $N = 4$ and we consider a regular reference tetrahedron (S_1, S_2, S_3, S_4) with center $O \in \mathbf{R}^3$ such that $\text{dist}(O, S_i) = 1$ and as before, we call $\mathbf{t}_i = \overrightarrow{OS_i}$ for $i = 1, 2, 3, 4$.

The position and orientation in the three dimensional space of the tetrahedron are described by the coordinates of the center $\mathbf{c} \in \mathbf{R}^3$ and a rotation $\mathcal{R} \in \text{SO}(3)$, in such a way that $d = 6$.

We place the center of the ball B_i at $\mathbf{x}_i = \mathbf{c} + \xi_i \mathcal{R} \mathbf{t}_i$ with $\xi_i > 0$ for $i = 1, 2, 3, 4$ as depicted in Fig. 2.3 and forbid possible rotation of the spheres around the axes. A global rotation ($\mathcal{R} \neq \mathbf{Id}$) of the swimmer is however allowed.

The four ball cluster is now completely described by the list of parameters $X = (\xi, \mathbf{c}, \mathcal{R}) \in \mathcal{S} \times \mathcal{P}$, where $\mathcal{S} := (\sqrt{\frac{3}{2}}, +\infty)^4$ and $\mathcal{P} = \mathbf{R}^3 \times \text{SO}(3)$. Again, the lower bound for ξ_i is chosen in order to avoid overlaps of the balls.

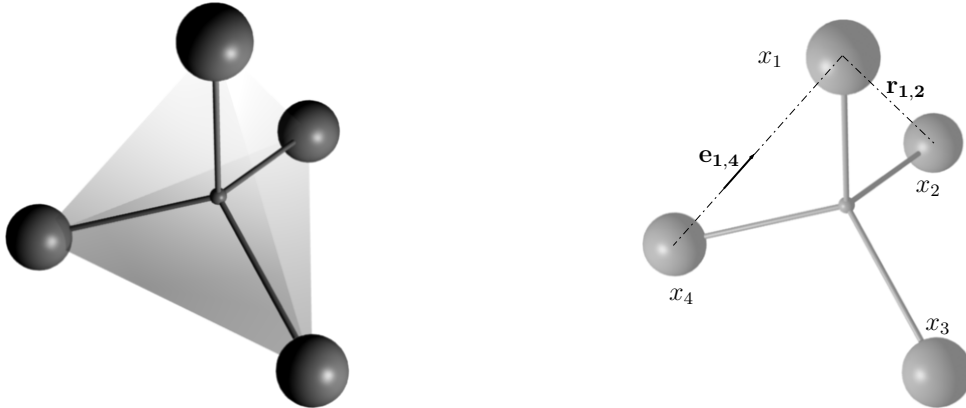


FIG. 2.3. *The four sphere swimmer (4S).*

Furthermore, the function \mathbf{X}_i are now defined as

$$\mathbf{X}_i(\xi, \mathbf{c}, \mathcal{R}, \mathbf{r}) = \mathbf{c} + \mathcal{R}(\xi_i \mathbf{t}_i + \mathbf{r}) \quad \forall i \in \{1, 2, 3, 4\},$$

which are still analytic in $(\xi, \mathbf{c}, \mathcal{R})$, from which we compute the instantaneous velocity on the sphere B_i

$$\mathbf{v}_i = \frac{\partial \mathbf{X}_i}{\partial t}(\xi, \mathbf{c}, \mathcal{R}, r) = \dot{\mathbf{c}} + \boldsymbol{\omega} \times (\xi_i \mathbf{t}_i + \mathbf{r}) + \mathcal{R} \mathbf{t}_i \dot{\xi}_i$$

where $\boldsymbol{\omega}$ is the angular velocity. Recall that $\boldsymbol{\omega} = Ax(\dot{\mathcal{R}}\mathcal{R})$ is the axial vector associated with the skew matrix $\dot{\mathcal{R}}\mathcal{R}$.

2.4. The result. In the theoretical part of this paper, we will establish the following theorem.

THEOREM 2.1. *Consider any of the swimmers described in Sections 2.1, 2.2 or 2.3, and assume it is self-propelled in a three dimensional infinite viscous flow modeled by Stokes equations. Then for any initial configuration $(\xi^i, p^i) \in \mathcal{S} \times \mathcal{P}$ any final configuration $(\xi^f, p^f) \in \mathcal{S} \times \mathcal{P}$ and any final time $T > 0$, there exists a stroke $\xi \in \mathcal{C}^0([0, T], \mathcal{S})$, piecewise $\mathcal{C}^1([0, T], \mathcal{S})$ satisfying $\xi(0) = \xi^i$ and $\xi(T) = \xi^f$ such that if the self-propelled swimmer starts in position p^i with the shape ξ^i at time $t = 0$, it ends at position p^f and shape ξ^f at time $t = T$ by changing its shape along $\xi(t)$.*

3. Modelization of the fluid. In this section we give the expression of the total force and torque induced by a shape change of the swimmer. Since the swimmer is composed of unions of balls, this turns out to study the Dirichlet-to-Neumann map outside the swimmer. We recall that the swimmer is composed of N identical and non-intersecting balls B_1, \dots, B_N of radius $a > 0$ not necessarily aligned, of center $\mathbf{x}_i \in \mathbf{R}^3$, but linked together by deformable jacks which form a kind of skeleton. Since the lateral size of the arms of this skeleton are negligible, we can consider that the fluid fills the unbounded domain $\Omega = \mathbf{R}^3 \setminus \cup_{i=1}^N \bar{B}_i$. Since the balls do not intersect, the vector $\mathbf{x} = (\mathbf{x}_1, \dots, \mathbf{x}_N) \in \Omega$ is restricted to belong to

$$\mathcal{S}_N := \left\{ \mathbf{x} \in (\mathbf{R}^3)^N : \min_{i < j} |\mathbf{x}_i - \mathbf{x}_j| > 2a \right\}.$$

We work at low Reynolds number, so that the fluid obeys Stokes equations

$$\begin{cases} -\eta \Delta \mathbf{u} + \nabla p &= 0 & \text{in } \Omega, \\ \nabla \cdot \mathbf{u} &= 0 & \text{in } \Omega, \\ -\boldsymbol{\sigma} \mathbf{n} &= \mathbf{f} & \text{on } \partial\Omega, \\ \mathbf{u} &\rightarrow 0 & \text{at } \infty. \end{cases} \quad (3.1)$$

where (\mathbf{u}, p) are respectively the velocity and the pressure of the fluid, η its viscosity, $\boldsymbol{\sigma} := \eta(\nabla \mathbf{u} + \nabla \mathbf{u}^t) - p \mathbf{Id}$ is the Cauchy stress tensor and \mathbf{n} is the outer unit normal to $\partial\Omega$ (hence, \mathbf{n} points from the fluid to the interior of the balls). Existence and uniqueness of a solution to (3.1) is classical in the Hilbert space

$$\mathcal{V} := \left\{ \mathbf{u} \in \mathcal{D}'(\Omega, \mathbf{R}^3) \mid \nabla \mathbf{u} \in L^2(\Omega), \frac{\mathbf{u}}{\sqrt{1 + |\mathbf{r}|^2}} \in L^2(\Omega) \right\},$$

endowed with the norm

$$\|\mathbf{u}\|_{\mathcal{V}}^2 := \int_{\Omega} |\nabla \mathbf{u}|^2.$$

Assuming that the force field belongs to $\mathcal{H}^{-1/2}(\partial\Omega)^1$, the solution of (3.1) can be expressed in terms of the associated Green's function, namely the stokeslet

$$\mathbf{G}(\mathbf{r}) := \frac{1}{8\pi\eta} \left(\frac{1}{|\mathbf{r}|} + \frac{\mathbf{r} \otimes \mathbf{r}}{|\mathbf{r}|^3} \right) \quad (3.2)$$

¹Here, and in all the paper the symbol \mathcal{H}^s denotes the Sobolev space of order s .

as

$$\mathbf{u}(\mathbf{r}) = \int_{\partial\Omega} \mathbf{G}(\mathbf{r} - \sigma) \mathbf{f}(\sigma) d\sigma \quad (3.3)$$

where \mathbf{f} is a distribution of forces on $\partial\Omega$. The Neumann-to-Dirichlet map

$$\begin{aligned} \mathcal{T} : \mathcal{H}^{-1/2}(\partial\Omega) &\longrightarrow \mathcal{H}^{1/2}(\partial\Omega) \\ \mathbf{f} &\longmapsto \mathbf{u}|_{\partial\Omega} = \left(\int_{\partial\Omega} \mathbf{G}(\mathbf{r} - \sigma) \mathbf{f}(\sigma) d\sigma \right)_{|\partial\Omega} \end{aligned} \quad (3.4)$$

is a one to one mapping onto while, by the open mapping Theorem, its inverse (the Dirichlet-to Neumann map) \mathcal{T}^{-1} is continuous.

Calling $B = B(O, a)$ the ball of radius a centered in the origin O , the special structure of our domain allows us to identify $\partial\Omega$ with $(\partial B)^N$ in such a way that \mathcal{T} can be seen as a map

$$\begin{aligned} \mathcal{T}_{\mathbf{x}} : \mathcal{H}_N^{-1/2} &\longrightarrow \mathcal{H}_N^{1/2} \\ (\mathbf{f}_1, \dots, \mathbf{f}_N) &\longmapsto (\mathbf{u}_1, \dots, \mathbf{u}_N) \end{aligned} \quad (3.5)$$

in which \mathcal{H}_N^s stands for $(\mathcal{H}^s(\partial B))^N$ and the dependence on $\mathbf{x} \in \mathcal{S}_N$ has been emphasized, defined by

$$\begin{aligned} \mathbf{u}_i(\mathbf{r}) &= \sum_{j=1}^N \int_{\partial B} \mathbf{G}(\mathbf{x}_i - \mathbf{x}_j + \mathbf{r} - \sigma) \mathbf{f}_j(\sigma) d\sigma \\ &=: \sum_{j=1}^N \langle \mathbf{f}_j, \mathbf{G}(\mathbf{x}_i - \mathbf{x}_j + \mathbf{r} - \cdot) \rangle_{\partial B}, \quad \mathbf{r} \in \partial B. \end{aligned} \quad (3.6)$$

3.1. Analyticity of the Dirichlet-to-Neumann map. This section is devoted to the following lemma which will be essential in the proof of the controllability theorem. This kind of result was already proved in [3] but with a much more complicated method. We therefore give another much simpler proof which applies to more general situations, e.g., the swimmers described in subsections 2.2 and 2.3. We denote by $\mathcal{L}(E, F)$ the Banach space of linear maps from E to F endowed with its usual norm.

LEMMA 3.1. *The mapping $\mathbf{x} \mapsto \mathcal{T}_{\mathbf{x}}$ is analytic from \mathcal{S}_N into $\mathcal{L}(\mathcal{H}_N^{-1/2}, \mathcal{H}_N^{1/2})$.*

The notion of analyticity in a Banach space is classical: it means that at all points $\mathbf{x}_0 \in \mathcal{S}_N$, $\mathcal{T}_{\mathbf{x}}$ is equal to its Taylor series which converges in $\mathcal{L}(\mathcal{H}_N^{-1/2}, \mathcal{H}_N^{1/2})$ for all \mathbf{x} in a suitable neighborhood of \mathbf{x}_0 .

Proof of Lemma 3.1

Let $\mathbf{x} \in \mathcal{S}_N$. From (3.6), we have for all $\mathbf{f} = (\mathbf{f}_1, \dots, \mathbf{f}_N) \in \mathcal{H}_N^{-1/2}$ and for all $i \in \{1, \dots, N\}$

$$(\mathcal{T}_{\mathbf{x}} \mathbf{f})_i(r) = \langle \mathbf{f}_i, \mathbf{G}(\mathbf{r} - \cdot) \rangle_{\partial B} + \sum_{j \neq i} \langle \mathbf{f}_j, \mathbf{G}(\mathbf{x}_i - \mathbf{x}_j + \mathbf{r} - \cdot) \rangle_{\partial B}.$$

Since the first term does not depend on \mathbf{x} , we only need to prove the analyticity of

$$\begin{aligned} \Psi : \mathbf{R}^3 \setminus 2B &\longrightarrow \mathcal{L}(\mathcal{H}^{-1/2}(\partial B), \mathcal{H}^{1/2}(\partial B)), \\ \mathbf{z} &\longmapsto \left(\mathbf{f} \mapsto \mathbf{g}(\mathbf{r}) := \langle \mathbf{f}, \mathbf{G}(\mathbf{z} + \mathbf{r} - \cdot) \rangle_{\partial B} \right) \end{aligned}$$

which follows from the analyticity of \mathbf{G} in $\mathbf{R}^3 \setminus \{0\}$ since this formula does not involve the singularity of the Green kernel \mathbf{G} . \square

We have the following consequence.

COROLLARY 1. *Since $\mathcal{T}_{\mathbf{x}}$ is an isomorphism for every $\mathbf{x} \in \mathcal{S}_N$, the mapping $\mathbf{x} \mapsto \mathcal{T}_{\mathbf{x}}^{-1}$ is also analytic from \mathcal{S}_N to $\mathcal{L}(\mathcal{H}_N^{1/2}, \mathcal{H}_N^{-1/2})$.*

Proof

For $\mathbf{x} \in \mathcal{S}_N$ and for $|\mathbf{y}|$ small enough, writing the Taylor series of $\mathcal{T}_{\mathbf{x}+\mathbf{y}}$ as

$$\mathcal{T}_{\mathbf{x}+\mathbf{y}} = \mathcal{T}_{\mathbf{x}} + \sum_{q \geq 1} \mathcal{T}_{\mathbf{x},q}(\mathbf{y}),$$

where $\mathcal{T}_{\mathbf{x},q}(\mathbf{y})$ denotes the q -homogeneous term in \mathbf{y} of $\mathcal{T}_{\mathbf{x}+\mathbf{y}}$, we have

$$\mathcal{T}_{\mathbf{x}+\mathbf{y}}^{-1} = \left\{ \left(Id + \sum_{q \geq 1} \mathcal{T}_{\mathbf{x},q}(\mathbf{y}) \mathcal{T}_{\mathbf{x}}^{-1} \right) \mathcal{T}_{\mathbf{x}} \right\}^{-1} = \mathcal{T}_{\mathbf{x}}^{-1} \left\{ \sum_{p \geq 0} (-1)^p \left(\sum_{q \geq 1} \mathcal{T}_{\mathbf{x},q}(\mathbf{y}) \mathcal{T}_{\mathbf{x}}^{-1} \right)^p \right\}$$

where the last expression may be rearranged as a converging Taylor series. \square

3.2. Approximation for large distances. We will also use the asymptotic behavior of $\mathcal{T}_{\mathbf{x}}^{-1}$ as $\delta(\mathbf{x}) := \min_{i < j} |\mathbf{x}_i - \mathbf{x}_j|$ tends to ∞ . For $i, j \in \{1, \dots, N\}$, we introduce the notation

$$\mathbf{x}_{i,j} := \mathbf{x}_i - \mathbf{x}_j, \quad r_{i,j} := |\mathbf{x}_{i,j}| \quad \text{and} \quad \mathbf{e}_{i,j} := \frac{\mathbf{x}_{i,j}}{r_{i,j}},$$

and, for every $\mathbf{f} \in \mathcal{H}^{-1/2}(\partial B, \mathbf{R}^3)$,

$$(\overline{\mathcal{T}}\mathbf{f})(\mathbf{r}) = \int_{\partial B} \mathbf{G}(\mathbf{r} - \sigma) \mathbf{f}(\sigma) d\sigma, \quad \forall \mathbf{r} \in \partial B.$$

PROPOSITION 3.2. *For every $\mathbf{f} \in \mathcal{H}_N^{-1/2}$,*

$$(\mathcal{T}_{\mathbf{x}}\mathbf{f})_i = \overline{\mathcal{T}}\mathbf{f}_i + \frac{1}{8\pi\eta} \sum_{j \neq i} \frac{1}{r_{i,j}} (\mathbf{Id} + \mathbf{e}_{i,j} \otimes \mathbf{e}_{i,j}) \langle \mathbf{f}_j, \mathbf{Id} \rangle_{\partial B} + O(\delta^{-2}) \|\mathbf{f}\|_{\mathcal{H}_N^{-1/2}}. \quad (3.7)$$

For every $\mathbf{g} \in \mathcal{H}_N^{1/2}$, $\mathbf{x} \in \mathcal{S}_N$ and $\mathbf{y} \in (\mathbf{R}^3)^N$, we have

$$(\mathcal{T}_{\mathbf{x}}^{-1}\mathbf{g})_i = \overline{\mathcal{T}}^{-1} \left\{ \mathbf{g}_i - \frac{1}{8\pi\eta} \sum_{j \neq i} \frac{1}{r_{i,j}} (\mathbf{Id} + \mathbf{e}_{i,j} \otimes \mathbf{e}_{i,j}) \langle \overline{\mathcal{T}}^{-1}\mathbf{g}_j, \mathbf{Id} \rangle_{\partial B} \right\} + O(\delta^{-2}) \|\mathbf{g}\|_{\mathcal{H}_N^{1/2}}. \quad (3.8)$$

Proof

Let $\mathbf{x} \in \mathcal{S}_N$ and $\mathbf{f} \in \mathcal{H}_N^{-1/2}$. From (3.6) we have for $i = 1, \dots, N$ and $\mathbf{r} \in \partial B$,

$$(\mathcal{T}_{\mathbf{x}}\mathbf{f})_i(\mathbf{r}) = \overline{\mathcal{T}}\mathbf{f}_i(\mathbf{r}) + \sum_{j \neq i} \langle \mathbf{f}_j, \mathbf{G}(\mathbf{x}_{i,j} + \mathbf{r} - \cdot) \rangle_{\partial B}. \quad (3.9)$$

Using the expansion

$$\mathbf{G}(\mathbf{x}_{i,j} + \mathbf{z}) = \mathbf{G}(\mathbf{x}_{i,j}) + O(\delta^{-2}),$$

which is valid uniformly for bounded \mathbf{z} , we get

$$\langle \mathbf{f}_j, \mathbf{G}(\mathbf{x}_{i,j} + \mathbf{r} - \cdot) \rangle_{\partial B} = \mathbf{G}(\mathbf{x}_{i,j}) \langle \mathbf{f}_j, \mathbf{Id} \rangle_{\partial B} + O(\delta^{-2}) \|\mathbf{f}\|_{\mathcal{H}_N^{-1/2}}.$$

Substituting into (3.9), and using (3.2), we obtain (3.7). For (3.8) we remark that (3.7) is the asymptotic expansion in \mathbf{x} of the analytic operator $\mathcal{T}_{\mathbf{x}}$ at infinity. Since $\overline{\mathcal{T}}$ is invertible, we obtain the expansion (3.8) by inverting (3.7). \square

In the sequel, we will use furthermore the fact that the spheres are non-deformable and may thus only move following a rigid body motion. In this case, the velocity of each point \mathbf{r} of the i -th sphere is given by

$$\mathbf{v}_i(\mathbf{r}) = \mathbf{u}_i + \omega_i \times \mathbf{r}. \quad (3.10)$$

Using (3.8) we find the expansion of the total force that the system applies to the fluid

$$\mathbf{F} = \sum_{i=1}^N 6\pi\eta a \mathbf{u}_i - \frac{9\pi\eta a^2}{2} \sum_{i=1}^N \sum_{j \neq i} \mathbf{S}_{ij} \mathbf{u}_j + O(\delta^{-2}) \|\mathbf{u}\|, \quad (3.11)$$

where \mathbf{S}_{ij} is the matrix defined by

$$\mathbf{S}_{ij} = \frac{1}{r_{i,j}} (\mathbf{Id} + \mathbf{e}_{i,j} \otimes \mathbf{e}_{i,j}), \quad (3.12)$$

while the total torque (with respect to the origin O) is given by

$$\mathbf{T} = 6\pi\eta a \sum_{i=1}^N \mathbf{x}_i \times \mathbf{u}_i + O(1) \|\mathbf{u}\|. \quad (3.13)$$

4. The swimming problem as an affine control problem without drift.

In this section we show that self-propulsion of the swimmers makes the system that describes their dynamics a linear control system.

LEMMA 4.1. *The system that describes the dynamics of low Re swimmers can be written in the form*

$$\frac{d}{dt} \begin{pmatrix} \xi \\ p \end{pmatrix} = \sum_{i=1}^M \mathbf{F}_i(\xi, p) \dot{\xi}_i, \quad (4.1)$$

where the vectorfields $(\mathbf{F}_i)_{1 \leq i \leq M}$ are analytic in (ξ, p) . It is therefore an affine control problem without drift where the controls are the rate of shape changes.

The rest of this section is devoted to the proof of this lemma. This can be seen as a generalization of the result obtained in [3] for the three sphere swimmer of Najafi and Golestanian. We show in particular how self-propulsion gives rise to the specific form (4.1) of the equation, describing the dynamics of all these swimmers of Section 2.

4.1. Self-propulsion. The question we want to address is whether it is possible to control the state of the system (i.e. both ξ and p) using as controls only the rate of shape changes $\dot{\xi}$. For this aim, we need to understand the way p varies when one changes ξ . This is done assuming that the swimmer is self-propelled, and that the swimmer's inertia is negligible, which implies that the total viscous force and torque exerted by the surrounding fluid on the swimmer must vanish. As we shall see, using these conditions, \dot{p} is uniquely and linearly determined by $\dot{\xi}$. The condition that total viscous force and torque vanish is written as

$$\sum_{i=1}^N \int_{\partial B} \mathcal{T}_{\mathbf{x}(\xi,p)}^{-1} \mathbf{v}_i(\xi, p, \mathbf{r}) d\sigma(\mathbf{r}) = 0, \quad (4.2)$$

and

$$\sum_{i=1}^N \int_{\partial B} \mathbf{X}_i(\xi, p, \mathbf{r}) \times \mathcal{T}_{\mathbf{x}(\xi,p)}^{-1} \mathbf{v}_i(\xi, p, \mathbf{r}) d\sigma(\mathbf{r}) = 0, \quad (4.3)$$

which lead, using (2.1), to a set of linear equations which link \dot{p} to $\dot{\xi}$. In all the examples we have in mind (see below), this allows us to solve \dot{p} uniquely and linearly in terms of $\dot{\xi}$

$$\dot{p} = \sum_{i=1}^M \mathbf{W}_i(\xi, p) \dot{\xi}_i. \quad (4.4)$$

In the preceding equation $(\mathbf{V}_i(\xi, p))_{1 \leq i \leq M}$ are M vector fields defined on $T\mathcal{P}$, the tangent bundle of \mathcal{P} .

The state of the system (ξ, p) thus follows the ODE

$$\begin{pmatrix} \dot{\xi} \\ \dot{p} \end{pmatrix} = \sum_{i=1}^M \mathbf{F}_i(\xi, p) \dot{\xi}_i, \quad (4.5)$$

where now for all $1 \leq i \leq M$, $\mathbf{F}_i(\xi, p) = \begin{pmatrix} \mathbf{e}_i \\ \mathbf{W}_i(\xi, p) \end{pmatrix}$ is a vector field defined on $T\mathcal{S} \times T\mathcal{P}$ (here \mathbf{e}_i is the i -th vector of the canonical basis of \mathbf{R}^M).

4.2. The three sphere swimmer of Najafi and Golestanian (3S). Due to axial symmetry, the only non trivial equation in (4.2) is the one concerning the component of the total viscous force along the axis of symmetry. This reads

$$\sum_{k=1}^2 \lambda_k(\xi, p) \dot{\xi}_k + \lambda_0(\xi, p) \dot{p} = 0,$$

where

$$\begin{aligned} \lambda_1(\xi) &= \sum_{i=1}^3 \int_{\partial B} \mathbf{e}_1 \cdot \left(\mathcal{T}_{\mathbf{x}(\xi,p)}^{-1} \left(\frac{\partial \mathbf{X}_1}{\partial \xi_1}, \frac{\partial \mathbf{X}_2}{\partial \xi_1}, \frac{\partial \mathbf{X}_3}{\partial \xi_1} \right) \right)_i d\mathbf{r} \\ &= \sum_{i=1}^3 \int_{\partial B} \frac{\partial \mathbf{X}_i}{\partial \xi_1} \cdot \left(\mathcal{T}_{\mathbf{x}(\xi,p)}^{-1} (\mathbf{e}_1, \mathbf{e}_1, \mathbf{e}_1) \right)_i d\mathbf{r} \\ &= - \int_{\partial B} \mathbf{e}_1 \cdot \left(\mathcal{T}_{\mathbf{x}(\xi,p)}^{-1} (\mathbf{e}_1, \mathbf{e}_1, \mathbf{e}_1) \right)_1 d\mathbf{r}, \end{aligned}$$

and, similarly,

$$\lambda_2(\xi) = \int_{\partial B} \mathbf{e}_1 \cdot \left(\mathcal{T}_{\mathbf{x}(\xi,p)}^{-1}(\mathbf{e}_1, \mathbf{e}_1, \mathbf{e}_1) \right)_3 d\mathbf{r},$$

while the coefficient of \dot{p} is simply given by

$$\begin{aligned} \lambda_0(\xi) &= \sum_{i=1}^3 \int_{\partial B} \mathbf{e}_1 \cdot \left(\mathcal{T}_{\mathbf{x}(\xi,p)}^{-1}(\mathbf{e}_1, \mathbf{e}_1, \mathbf{e}_1) \right)_i d\mathbf{r} \\ &> 0. \end{aligned}$$

Positivity of the viscous drag λ_0 arising from a rigid translation at unit speed is a consequence of the positive-definiteness of the Oseen resistance matrix, see [17]. The coefficients above are independent of p because of translational invariance of the problem. From the analyticity of the coefficients and $\mathcal{T}_{\mathbf{x}}$ in \mathbf{x} , we have that

$$\dot{p} = \sum_{k=1}^2 V_k(\xi) \dot{\xi}_k,$$

where $V_k(\xi) = -\frac{\lambda_k(\xi)}{\lambda_0(\xi)}$ are analytic functions of ξ_1, ξ_2 . The complete system reads

$$\frac{d}{dt} \begin{pmatrix} \xi \\ p \end{pmatrix} = \alpha_1(t) \begin{pmatrix} 1 \\ 0 \\ V_1(\xi) \end{pmatrix} + \alpha_2(t) \begin{pmatrix} 0 \\ 1 \\ V_2(\xi) \end{pmatrix} \quad (4.6)$$

where $\alpha_1(t) = \dot{\xi}_1(t)$ and $\alpha_2(t) = \dot{\xi}_2(t)$ are the control functions. This is under the form (4.1).

4.3. The three sphere swimmer moving in a plane (3SP). Due to the symmetries of the system, the swimmer stays in the horizontal plane. Therefore, the third component of the total force F_3 vanishes, while only the third component of the total torque T_3 might not vanish. The constraints of self-propulsion (4.2) and (4.3) – more precisely, the vanishing of the components F_1 , and F_2 of the force, and of the third component T_3 of the torque – lead to a linear system that can be written as

$$\mathbf{Res}(\xi, \theta) \begin{pmatrix} \dot{\mathbf{c}} \\ \dot{\theta} \end{pmatrix} + \sum_{i=1}^3 \mathbf{V}_i(\xi, \theta) \dot{\xi}_i = 0,$$

where neither \mathbf{Res} , nor \mathbf{V}_i depend on \mathbf{c} because of translational invariance of the Stokes problem.

The complete system reads

$$\begin{pmatrix} \dot{\xi} \\ \dot{\mathbf{c}} \\ \dot{\theta} \end{pmatrix} = \begin{pmatrix} \mathbf{Id} \\ -\mathbf{Res}^{-1}(\xi, \theta) \mathbf{V}(\xi, \theta) \end{pmatrix} \alpha(t), \quad (4.7)$$

where $\mathbf{V}(\xi, \theta)$ is the 3×3 matrix whose columns are $\mathbf{V}_i(\xi, \theta)$, and $\alpha(t) = \dot{\xi} \in \mathbf{R}^3$ are the controls. This is again under the form (4.1).

4.4. The four sphere swimmer moving in space (4S). Constraints of self propulsion (4.2) and (4.3) now become

$$\begin{pmatrix} \mathbf{K}(\xi, \mathcal{R}) & \mathbf{C}^T(\xi, \mathcal{R}) \\ \mathbf{C}(\xi, \mathcal{R}) & \mathbf{\Omega}(\xi, \mathcal{R}) \end{pmatrix} \begin{pmatrix} \dot{\xi} \\ \dot{\omega} \end{pmatrix} + \sum_{i=1}^4 \mathbf{V}_i(\xi, \mathcal{R}) \dot{\xi}_i = 0,$$

where the 6×6 matrix

$$\mathbf{Res}(\xi, \mathcal{R}) = \begin{pmatrix} \mathbf{K}(\xi, \mathcal{R}) & \mathbf{C}^T(\xi, \mathcal{R}) \\ \mathbf{C}(\xi, \mathcal{R}) & \mathbf{\Omega}(\xi, \mathcal{R}) \end{pmatrix} \quad (4.8)$$

known as the resistance matrix [17] is symmetric positive definite, and depends analytically on (ξ, \mathcal{R}) , just as the vectors $\mathbf{V}_i(\xi, \mathcal{R})$ do.

In this case, the complete system reads

$$\begin{pmatrix} \dot{\xi} \\ \dot{\mathbf{c}} \\ \dot{\omega} \end{pmatrix} = \begin{pmatrix} \mathbf{Id}_{4,4} \\ -\mathbf{Res}^{-1}(\xi, \mathcal{R}) \mathbf{V}(\xi, \mathcal{R}) \end{pmatrix} \alpha(t), \quad (4.9)$$

where $\mathbf{V}(\xi, \mathcal{R})$ is the 6×4 matrix whose columns are $\mathbf{V}_i(\xi, \mathcal{R})$, and $\alpha(t) \in \mathbf{R}^4$ are the controls. Using $\dot{\mathcal{R}} = \text{skew}(\omega)\mathcal{R}$ enables us to write the system under the more classical form (4.1)

$$\begin{pmatrix} \dot{\xi} \\ \dot{\mathbf{c}} \\ \dot{\mathcal{R}} \end{pmatrix} = \sum_{i=1}^4 \mathbf{F}_i(\xi, \mathcal{R}) \alpha_i(t), \quad (4.10)$$

where $\alpha_i(t) = \dot{\xi}_i(t)$ are the control functions.

5.1. Geometric control theory. When we use $(\dot{\xi}_i)_{1 \leq i \leq M}$ as control variables, systems like (4.5) belong to the class of linear control systems with analytic coefficients of the form

$$\frac{dX}{dt} = \sum_{i=1}^M \alpha_i(t) F_i(X) \quad (5.1)$$

where X is a point of a d -dimensional manifold \mathcal{M} , and $(F_i)_{1 \leq i \leq M}$ are p vector fields defined on $T\mathcal{M}$, the tangent bundle of \mathcal{M} . For such systems, the tools of geometric control theory can be applied. In our case, \mathcal{M} and the vector fields F_i are furthermore analytic, which enables us to use stronger results. The theory for such systems may be found in [1, 19], for instance.

In (5.1), the control which governs the system is the vector $(\alpha_1, \dots, \alpha_p)$, and the question of controllability of the system can be stated as follows:

QUESTION 1. *For any pair of states $(X_0, X_1) \in \mathcal{M}^2$, are there M functions $\alpha_i : [0, T] \rightarrow \mathbf{R}$ such that solving (5.1) starting from $X(0) = X_0$ leads to $X(T) = X_1$?*

A classical result by Rashevsky and Chow states that the system (5.1) is locally controllable near $X_0 \in \mathcal{M}$ (which means that question 1 possesses a positive answer for any X_1 in a suitable neighborhood of X_0) with piecewise constant controls α_i that

are moreover continuous from the right, if the Lie algebra generated by (F_1, \dots, F_M) is of full rank at X_0

$$\dim \text{Lie}(F_1, \dots, F_M)(X_0) = d. \quad (5.2)$$

Here, the Lie algebra $\text{Lie}(F_1, \dots, F_M)(X_0)$ is the algebra obtained from the vector fields (F_1, \dots, F_M) by successive applications of the Lie bracket operation defined as

$$[F, G](X) = (F \cdot \nabla)G(X) - (G \cdot \nabla)F(X).$$

The rigorous proof of Rashevsky-Chow's theorem may be found in [1, 19] but we would like to give here a hint of why such a result holds. Given a vector field $F : \mathcal{M} \rightarrow T\mathcal{M}$, we call $\exp(tF)(X_0)$ the solution at time t of

$$\begin{cases} \frac{dX}{dt} = F(X), \\ X(0) = X_0. \end{cases} \quad (5.3)$$

The main idea is that one can reach from X_0 points in the direction $g = \sum_i \beta_i F_i(X_0)$ by using (5.3) with $F = \sum_i \beta_i F_i$ since we have, to first order, for small $|t| \ll 1$,

$$\exp(tF)(X_0) = X_0 + tF(X_0) + O(t^2) = X_0 + tg + O(t^2).$$

This formula shows that the global displacement of the solution of the dynamical system is proportional to time for these directions.

A more subtle move allows one to reach points in the direction $[F_i, F_j]$. Namely, we now need to consider

$$\exp(-tF_i) \circ \exp(-tF_j) \circ \exp(tF_i) \circ \exp(tF_j)(X_0) = X_0 + t^2[F_i, F_j](X_0) + O(t^3),$$

which also shows that in time t , one can reach a displacement in the desired direction which is proportional to t^2 . Lie bracket directions of higher order are also attainable at the price of higher order expressions in t , leading to smaller displacements. If the Lie algebra has a full rank, every direction in \mathcal{M} is attainable and the system is locally controllable.

We will focus on systems for which the full rank condition (5.2) is satisfied with first order Lie brackets only, and a necessary condition for

$$\dim \text{Span}(F_1, \dots, F_M, [F_1, F_2], [F_1, F_3], \dots, [F_{M-1}, F_M])(X_0) = d,$$

is that

$$M + \frac{M(M-1)}{2} \geq d.$$

Our three systems are designed in such a way that they all satisfy $M + \frac{M(M-1)}{2} = d$, and local controllability near X_0 follows from verifying that

$$\det(F_1, \dots, F_M, [F_1, F_2], [F_1, F_3], \dots, [F_{M-1}, F_M])(X_0) \neq 0. \quad (5.4)$$

The remaining of this section consists in the detailed analysis of our three model swimmers. In each case, we show that (5.4) holds at one point. proving local controllability at one point (ξ_0, p_0) . In order to obtain global controllability, and theorem 2.1, we need a special argument which is the aim of Section 5.5. The regularity of the shape function $\xi(t)$ follows from the fact that the controls are here the rate of shape changes.

5.2. The 3S swimmer. For the equation (4.6), the controllability condition (5.4) becomes

$$\det(F_1, F_2, [F_1, F_2])(\xi) = \frac{\partial V_2}{\partial \xi_1}(\xi) - \frac{\partial V_1}{\partial \xi_2}(\xi) \neq 0, \quad (5.5)$$

which is enough to verify for one configuration. For this purpose, and in order to further simplify the computation, we make the observation that, due to symmetry,

$$\lambda_1(\xi_1, \xi_2) = -\lambda_2(\xi_2, \xi_1), \text{ while } \lambda_0(\xi_1, \xi_2) = \lambda_0(\xi_2, \xi_1).$$

Therefore, if we consider a symmetric shape $\bar{\xi} = (\zeta, \zeta)$, showing that condition (5.5) holds at $\bar{\xi}$ is equivalent to proving that

$$\frac{\partial \lambda_1}{\partial \xi_2}(\bar{\xi}) \neq 0.$$

Using the expansion for large distances of the total force (3.11) with $\mathbf{u}_1 = (\dot{p} - \dot{\xi}_1)\mathbf{e}_1$, $\mathbf{u}_2 = \dot{p}\mathbf{e}_1$, and $\mathbf{u}_3 = (\dot{p} + \dot{\xi}_2)\mathbf{e}_1$, leads to

$$\begin{aligned} \lambda_0(\xi_1, \xi_2) &= 6\pi a\eta \left(3 - \frac{3a}{2} \left(\frac{1}{\xi_1} + \frac{1}{\xi_2} + \frac{1}{\xi_1 + \xi_2} \right) \right) + O(\zeta^{-2}), \\ \lambda_1(\xi_1, \xi_2) &= 6\pi a\eta \left(1 - \frac{3a}{2} \left(\frac{1}{\xi_1} + \frac{1}{\xi_1 + \xi_2} \right) \right) + O(\zeta^{-2}), \\ \lambda_2(\xi_1, \xi_2) &= 6\pi a\eta \left(-1 + \frac{3a}{2} \left(\frac{1}{\xi_2} + \frac{1}{\xi_1 + \xi_2} \right) \right) + O(\zeta^{-2}). \end{aligned}$$

Therefore

$$\frac{\partial \lambda_1}{\partial \xi_2}(\bar{\xi}) = \frac{9\pi a^2 \eta}{4\zeta^2} + O(\zeta^{-3})$$

which does not vanish for ζ sufficiently large. This proves the global controllability of the system.

5.3. The 3SP swimmer. We check the controllability condition (5.4) for the equation (4.7) at $\bar{\theta} = 0$ and at a symmetric shape $\bar{\xi} = (\zeta, \zeta, \zeta)$, with $\zeta \in \mathbf{R}$ sufficiently large.

Calling $\mathbf{F}_i = -\mathbf{Res}^{-1}(\xi, \theta)\mathbf{V}_i(\xi, \theta)$, the special form of our system (in particular the fact that the coefficients do not depend on the position variable \mathbf{c}) allows us to rewrite the sufficient condition (5.4) for controllability at $(\bar{\xi}, \mathbf{c}, \theta)$ as

$$\Delta = \det \left(\frac{\partial \mathbf{F}_1}{\partial \xi_2} - \frac{\partial \mathbf{F}_2}{\partial \xi_1}, \frac{\partial \mathbf{F}_2}{\partial \xi_3} - \frac{\partial \mathbf{F}_3}{\partial \xi_2}, \frac{\partial \mathbf{F}_3}{\partial \xi_1} - \frac{\partial \mathbf{F}_1}{\partial \xi_3} \right) (\bar{\xi}) \neq 0. \quad (5.6)$$

Notice that the absence of $\partial/\partial\theta$ terms come from the fact that $(\mathbf{F}_i)_3 = 0$ in a symmetric configuration. We now turn to the computation of $\frac{\partial \mathbf{F}_k}{\partial \xi_l}(\bar{\xi})$ for $k \neq l$ or, at least, of its asymptotic expansion in terms of negative powers of ζ .

From the definition of \mathbf{F}_k , one has

$$\frac{\partial \mathbf{F}_k}{\partial \xi_l} = -\mathbf{Res}^{-1}(\xi, \theta) \left(\frac{\partial \mathbf{V}_k}{\partial \xi_l} + \frac{\partial \mathbf{Res}}{\partial \xi_l} \mathbf{F}_k \right), \quad (5.7)$$

and we need to compute all the factors of this expression at $(\bar{\xi}, 0)$.

The first step consists in computing an expansion for $\mathbf{Res}(\bar{\xi}, 0)$. We get from (3.11) and (3.13), and taking $N = 3$,

$$\mathbf{Res}(\bar{\xi}, 0) = 6\pi a\eta \begin{pmatrix} 3\mathbf{Id} + O(\zeta^{-1}) & O(1) \\ O(1) & 3\zeta^2 + O(\zeta) \end{pmatrix}, \quad (5.8)$$

and

$$\mathbf{Res}^{-1}(\bar{\xi}, 0) = \frac{1}{6\pi a\eta} \begin{pmatrix} \frac{1}{3}\mathbf{Id} + O(\zeta^{-1}) & O(\zeta^{-2}) \\ O(\zeta^{-2}) & \frac{1}{3\zeta^2} + O(\zeta^{-3}) \end{pmatrix}. \quad (5.9)$$

Differentiating \mathbf{Res} with respect to ξ_l gives (notice that from Section 3.1, \mathbf{Res} is analytic in ξ and we may therefore differentiate its expansion term by term)

$$\frac{\partial \mathbf{Res}}{\partial \xi_l}(\bar{\xi}, 0) = 6\pi a\eta \begin{pmatrix} -\frac{3}{2}a \frac{\partial}{\partial \xi_l} \left(\sum_{i \neq l} \mathbf{S}_{il} \right) + O(\zeta^{-3}) & \mathbf{t}_l \times \mathbf{e}_3 + O(\zeta^{-1}) \\ (\mathbf{t}_l \times \mathbf{e}_3)^t + O(\zeta^{-1}) & O(\zeta) \end{pmatrix}, \quad (5.10)$$

where \mathbf{S}_{ij} , originally given by (3.12), is now seen as its restriction to the horizontal plane, and the vector $\mathbf{t}_l \times \mathbf{e}_3$ as a horizontal vector.

Similarly

$$\mathbf{V}_k(\bar{\xi}, 0) = \begin{pmatrix} 6\pi\eta a \mathbf{t}_k - 9\pi\eta a^2 \sum_{i \neq k} \mathbf{S}_{ik} \mathbf{t}_k + O(\zeta^{-2}) \\ O(1) \end{pmatrix} \quad (5.11)$$

gives

$$\mathbf{F}_k(\bar{\xi}, 0) = -\frac{1}{3} \begin{pmatrix} \mathbf{t}_k + O(\zeta^{-1}) \\ 0 \end{pmatrix} \quad (5.12)$$

(here we have used the fact that, for a symmetric configuration, the displacement of one sphere induces no torque) and

$$\frac{\partial \mathbf{V}_k}{\partial \xi_l}(\bar{\xi}, 0) = -9\pi\eta a^2 \begin{pmatrix} \frac{\partial \mathbf{S}_{lk}}{\partial \xi_l} \mathbf{t}_k + O(\zeta^{-3}) \\ O(\zeta^{-1}) \end{pmatrix}. \quad (5.13)$$

From these expressions, and using (5.7), and the identity

$$\frac{\partial \mathbf{S}_{il}}{\partial \xi_l} = \frac{1}{r_{il}^2} (-\mathbf{e}_{il} \cdot \mathbf{t}_l) \mathbf{Id} + \mathbf{t}_l \otimes \mathbf{e}_{il} + \mathbf{e}_{il} \otimes \mathbf{t}_l - 3(\mathbf{e}_{il} \cdot \mathbf{t}_l) \mathbf{e}_{il} \otimes \mathbf{e}_{il}$$

one gets (after some calculations)

$$\frac{\partial \mathbf{F}_k}{\partial \xi_l}(\bar{\xi}, 0) - \frac{\partial \mathbf{F}_l}{\partial \xi_k}(\bar{\xi}, 0) = \begin{pmatrix} \frac{4a}{\zeta^2} (\mathbf{t}_l - \mathbf{t}_k) \\ -\frac{1}{9\zeta^2} \mathbf{t}_l \times \mathbf{t}_k \cdot \mathbf{e}_3 \end{pmatrix} + O(\zeta^{-3}). \quad (5.14)$$

The determinant Δ given by (5.6) is thus equal to

$$\Delta = -\zeta^{-6} \frac{16a^2}{9} \det \begin{pmatrix} \mathbf{t}_2 - \mathbf{t}_1 & \mathbf{t}_3 - \mathbf{t}_2 & \mathbf{t}_1 - \mathbf{t}_3 \\ \mathbf{t}_2 \times \mathbf{t}_1 \cdot \mathbf{e}_3 & \mathbf{t}_3 \times \mathbf{t}_2 \cdot \mathbf{e}_3 & \mathbf{t}_1 \times \mathbf{t}_3 \cdot \mathbf{e}_3 \end{pmatrix} + O(\zeta^{-7})$$

which does not vanish for ζ large enough.

We emphasize again that the global controllability result proven here means that, by using suitable controls, the swimmer is capable of moving anywhere in the horizontal plane and of rotating around the vertical axis by any angle.

5.4. The 4S swimmer. As before, we check the controllability condition (5.4) for the equation (4.10) at a symmetric shape $\bar{\xi} = (\zeta, \zeta, \zeta, \zeta)$, with ζ sufficiently large. Also, we use $\mathcal{R} = \mathbf{Id}$ in the verification of the Lie bracket condition (5.4).

Notice that for the symmetric configuration $\bar{\xi}$, the vectors \mathbf{F}_i defined by (4.9,4.10), have no torque components, and that \mathbf{F}_i does not depend on \mathbf{c} because of the translational invariance of the problem. Taking into account these facts, the sufficient condition (5.4) for controllability at $(\bar{\xi}, 0, \mathbf{Id})$ simplifies to

$$\dim \text{Span} \left(\frac{\partial \mathbf{F}_1}{\partial \xi_2} - \frac{\partial \mathbf{F}_2}{\partial \xi_1}, \dots, \frac{\partial \mathbf{F}_3}{\partial \xi_4} - \frac{\partial \mathbf{F}_4}{\partial \xi_3} \right) (\bar{\xi}, \mathbf{Id}) = 6. \quad (5.15)$$

Notice that in the preceding equation, each vector is a tangent vector to the group of 3 dimensional rigid transformations, $SE(3) = \mathbb{R}^3 \times SO(3)$. In order to simplify the computation, it is convenient to call $\phi_i = -\mathbf{Res}^{-1}(\bar{\xi}, \mathcal{R})\mathbf{V}_i$ (see (4.9)), and work in *translations and angular velocities*. A simple change of coordinates shows that condition (5.15) simply rewrites

$$\Delta = \det \left(\frac{\partial \phi_1}{\partial \xi_2} - \frac{\partial \phi_2}{\partial \xi_1}, \dots, \frac{\partial \phi_3}{\partial \xi_4} - \frac{\partial \phi_4}{\partial \xi_3} \right) (\bar{\xi}, \mathbf{Id}) \neq 0. \quad (5.16)$$

We now turn to the computation of $\frac{\partial \phi_k}{\partial \xi_l}(\bar{\xi}, \mathbf{Id})$ for $k \neq l$, or at least of its asymptotic expansion in terms of negative powers of ζ .

The definition of ϕ_k still gives

$$\frac{\partial \phi_k}{\partial \xi_l} = -\mathbf{Res}^{-1}(\bar{\xi}, \mathcal{R}) \left(\frac{\partial \mathbf{V}_k}{\partial \xi_l} + \frac{\partial \mathbf{Res}}{\partial \xi_l} \phi_k \right), \quad (5.17)$$

and we need to compute all the factors of this expression at $(\bar{\xi}, \mathbf{Id})$.

The first step consists in computing an expansion of $\mathbf{Res}(\bar{\xi}, \mathbf{Id})$. We have from (3.11) and (3.13)

$$\begin{aligned} \mathbf{K} &= 6\pi a\eta N \mathbf{Id} - \frac{9\pi\eta a^2}{2} \sum_{i=1}^N \sum_{j \neq i}^N \mathbf{S}_{ij} + O(\zeta^{-2}), \\ \mathbf{C} &= 6\pi a\eta \sum_{i=1}^N \xi_i \text{skew}(\mathbf{t}_i) + O(\zeta^0), \text{ with } \text{skew}(\mathbf{t})\mathbf{x} = \mathbf{t} \times \mathbf{x}, \forall \mathbf{x} \in \mathbf{R}^3, \\ \mathbf{\Omega} &= 6\pi a\eta \sum_{i=1}^N \xi_i^2 (\mathbf{Id} - \mathbf{t}_i \otimes \mathbf{t}_i) + O(\zeta). \end{aligned}$$

This gives (here $N = 4$, $\sum_{i=1}^4 \mathbf{t}_i = 0$ and $\sum_{i=1}^4 (\mathbf{Id} - \mathbf{t}_i \otimes \mathbf{t}_i) = \frac{8}{3} \mathbf{Id}$)

$$\mathbf{Res}(\bar{\xi}, \mathbf{Id}) = 6\pi a\eta \begin{pmatrix} 4\mathbf{Id} + O(\zeta^{-1}) & O(\zeta^{-1}) \\ O(\zeta^{-1}) & \frac{8\zeta^2}{3} \mathbf{Id} + O(\zeta) \end{pmatrix}, \quad (5.18)$$

and

$$\mathbf{Res}^{-1}(\bar{\xi}, \mathbf{Id}) = \frac{1}{6\pi a\eta} \begin{pmatrix} \frac{1}{4} \mathbf{Id} + O(\zeta^{-1}) & O(\zeta^{-2}) \\ O(\zeta^{-2}) & \frac{3}{8\zeta^2} \mathbf{Id} + O(\zeta^{-3}) \end{pmatrix}. \quad (5.19)$$

Differentiating \mathbf{Res} with respect to ξ_l gives (notice that from Section 3.1, \mathbf{Res} is analytic in ξ and we may therefore differentiate its expansion term by term)

$$\frac{\partial \mathbf{Res}}{\partial \xi_l}(\bar{\xi}, \mathbf{Id}) = 6\pi a \eta \begin{pmatrix} -\frac{3}{2}a \frac{\partial}{\partial \xi_l} \left(\sum_{i \neq l} \mathbf{S}_{il} \right) + O(\zeta^{-3}) & -\text{skew}(\mathbf{t}_l) + O(\zeta^{-1}) \\ \text{skew}(\mathbf{t}_l) + O(\zeta^{-1}) & O(\zeta) \end{pmatrix}. \quad (5.20)$$

Similarly

$$\mathbf{V}_k = \begin{pmatrix} 6\pi \eta a \mathbf{t}_k - 9\pi \eta a^2 \sum_{i \neq k} \mathbf{S}_{ik} \mathbf{t}_k + O(\zeta^{-2}) \\ O(1) \end{pmatrix} \quad (5.21)$$

leads to

$$\phi_k(\bar{\xi}, \mathbf{Id}) = -\frac{1}{4} \begin{pmatrix} \mathbf{t}_k + O(\zeta^{-1}) \\ 0 \end{pmatrix} \quad (5.22)$$

(here we have used the fact that for a symmetric configuration, the displacement of one sphere induces no torque) and

$$\frac{\partial \mathbf{V}_k}{\partial \xi_l}(\bar{\xi}, \mathbf{Id}) = -9\pi \eta a^2 \begin{pmatrix} \frac{\partial \mathbf{S}_{lk}}{\partial \xi_l} \mathbf{t}_k + O(\zeta^{-3}) \\ O(\zeta^{-1}) \end{pmatrix}. \quad (5.23)$$

From these expressions, and using (5.17), one gets after a tedious but straightforward computation

$$\frac{\partial \phi_k}{\partial \xi_l}(\bar{\xi}, \mathbf{Id}) - \frac{\partial \phi_l}{\partial \xi_k}(\bar{\xi}, \mathbf{Id}) = \begin{pmatrix} \frac{9\sqrt{3}a}{64\sqrt{2}\zeta^2} (\mathbf{t}_l - \mathbf{t}_k) \\ \frac{3}{16\zeta^2} \mathbf{t}_l \times \mathbf{t}_k \end{pmatrix} + O(\zeta^{-3}). \quad (5.24)$$

The determinant Δ given by (5.16) is thus equal to

$$\Delta = \zeta^{-12} \left(\frac{27\sqrt{3}a}{1024\sqrt{2}} \right)^3 \det \begin{pmatrix} \mathbf{t}_2 - \mathbf{t}_1 & \mathbf{t}_3 - \mathbf{t}_1 & \cdots & \mathbf{t}_4 - \mathbf{t}_3 \\ \mathbf{t}_2 \times \mathbf{t}_1 & \mathbf{t}_3 \times \mathbf{t}_1 & \cdots & \mathbf{t}_4 \times \mathbf{t}_3 \end{pmatrix} + O(\zeta^{-13})$$

which does not vanish for ζ large enough.

5.5. From local to global controllability. In all the three model swimmers that we proposed, we have found a point $(\xi_0, p_0) \in \mathcal{S} \times \mathcal{P}$ at which the sufficient condition for local controllability

$$\det(\mathbf{F}_1, \dots, \mathbf{F}_M, [\mathbf{F}_1, \mathbf{F}_2], \dots, [\mathbf{F}_{M-1}, \mathbf{F}_M]) (\xi_0, p_0) \neq 0, \quad (5.25)$$

holds, which proves, denoting by \mathcal{F} the family of analytic vector-fields $(\mathbf{F}_1, \dots, \mathbf{F}_M)$, that

$$\dim \text{Lie}_{(\xi_0, p_0)}(\mathcal{F}) = M + \frac{M(M-1)}{2} = d.$$

In order to show the global controllability of the problem, we show the following lemma

LEMMA 5.1. *For every $(\xi, p) \in \mathcal{S} \times \mathcal{P}$,*

$$\dim \text{Lie}_{(\xi, p)}(\mathcal{F}) = d. \quad (5.26)$$

Proof

Let $(\xi, p) \in \mathcal{S} \times \mathcal{P}$. From Hermann-Nagano Theorem (see [19], p. 48), we know that (5.26) holds at every point $(\bar{\xi}, \bar{p})$ in the orbit $\mathcal{O}_{\mathcal{F}}(\xi_0, p_0)$ of \mathcal{F} passing through (ξ_0, p_0) . Now, due to the specific form of the $(\mathbf{F}_i)_{1 \leq i \leq M}$, there exists $q \in \mathcal{P}$ such that $(\xi, q) \in \mathcal{O}_{\mathcal{F}}(\xi_0, p_0)$. Indeed,

$$(\xi, q) = \exp \left(\sum_{i=1}^M (\xi - \xi_0)_i \mathbf{F}_i \right) (\xi_0, p_0).$$

Eventually, because of the invariance of the problem with respect to the orientation of the swimmer, one has

$$\dim \text{Lie}_{(\xi, p)}(\mathcal{F}) = \dim \text{Lie}_{(\xi, q)}(\mathcal{F}) = \dim \text{Lie}_{(\xi_0, p_0)}(\mathcal{F}) = d.$$

This ends the proof of Lemma 5.1 and thus of Theorem 2.1. \square

6. Optimal swimming. A possible notion of optimal swimming consists in minimizing the energy dissipated while trying to reach a given position p_T at time T from an initial position p_0 at time 0. In this sense, the optimal stroke is the one that minimizes

$$\mathcal{E}(\xi, p) := \int_0^T \sum_{i=1}^N \sum_{j=1}^N \int_{\partial B} \mathbf{v}_i(\xi, p, \mathbf{r}) \cdot \mathcal{T}_{\mathbf{x}(\xi, p)}^{-1} \mathbf{v}_j(\xi, p, \mathbf{r}) d\sigma(\mathbf{r}) dt \quad (6.1)$$

where \mathbf{v} satisfies the self-propulsion conditions expressed by Equations (4.2) and (4.3), subject to the constraint that $p(T)$ is equal to p_T .

The special structure of our problem allows us to express the dissipated energy solely in terms of the shape variables ξ , by virtue of equation (4.4). We start by expressing the velocity of the m -th ball due to a unit shape change in the i -th component of $\dot{\xi}$ as

$$\mathbf{w}_i^m(\xi, p, \mathbf{r}) := \nabla_{\xi} \mathbf{X}_m(\xi, p, \mathbf{r}) \cdot \mathbf{e}_i + \nabla_p \mathbf{X}_m(\xi, p, \mathbf{r}) \cdot (\mathbf{V}(\xi, p) \cdot \mathbf{e}_i). \quad (6.2)$$

This allows us to simplify the energy of the system to an expression depending on the rate of shape and position changes $\dot{\xi}$:

$$\mathcal{E}(\xi, p) := \int_0^T \sum_{i=1}^M \sum_{j=1}^M \dot{\xi}_i \mathcal{G}_{ij}(\xi, p) \dot{\xi}_j dt, \quad (6.3)$$

where the metric \mathcal{G} is defined by

$$\mathcal{G}_{ij}(\xi, p) := \sum_{m=1}^N \int_{\partial B} \mathbf{w}_i^m(\xi, p, \mathbf{r}) \cdot \mathcal{T}_{\mathbf{x}(\xi, p)}^{-1} (\mathbf{w}_j^1(\xi, p, \mathbf{r}), \dots, \mathbf{w}_j^N(\xi, p, \mathbf{r}))^m d\sigma(\mathbf{r}). \quad (6.4)$$

Since dissipation is invariant with respect to the current position p , it is possible to show that $\mathcal{G}_{ij}(\xi, p) = \mathcal{G}_{ij}(\xi, 0) := \mathcal{G}_{ij}(\xi)$ for any position p .

Optimal swimming is then given by the solution $(\bar{\xi}, \bar{p}) : [0, T] \rightarrow \mathcal{S} \times \mathcal{P}$ of

$$\min_{(\xi, p) \in (\mathcal{S} \times \mathcal{P})} \int_0^T \dot{\xi} \cdot \mathcal{G}(\xi) \cdot \dot{\xi} dt =: \mathcal{E}(\xi) \quad (6.5a)$$

$$\text{subject to } C(\xi, p, t) = 0 \quad \forall t \in [0, T] \quad (6.5b)$$

$$\xi_L \leq \xi(t) \leq \xi_U \quad \forall t \in [0, T], \quad (6.5c)$$

where the constraints $C(\xi, p, t) = 0$ are given explicitly by

$$\begin{aligned}
\mathbf{V}(\xi(t), p(t)) \cdot \dot{\xi}(t) - \dot{p}(t) &= 0, & \forall t \in [0, T], \\
\xi(0) - \xi(T) &= 0, \\
p(0) - p_0 &= 0, \\
p(T) - p_T &= 0, \\
\xi(0) - \xi_0 &= 0.
\end{aligned} \tag{6.6}$$

Some of the constraints in (6.6) can be relaxed. For example, it is possible to fix only the periodicity of the shape, but not its actual initial and final values (so that the last constraint in (6.6) disappears), or to fix only some of the components of $p(T)$, leaving the others free to be optimized.

7. Numerical Approximation. Our strategy for the solution to problem (6.5) is to discretize in time both $\xi(t)$ and $p(t)$ using cubic splines, and rewrite everything as a finite dimensional constrained optimization problem, defined only on the coefficients of the spline approximation of ξ and p .

A C++ code for boundary integral methods, which has been developed using the `deal.II` library (see [8] and [7]), solves the Dirichlet-to-Neumann map \mathcal{T}^{-1} , and is then used to construct $\mathcal{G}(\xi)$ and $\mathbf{V}(\xi, p)$.

The finite element method in the spline space is then used to produce a finite dimensional approximation to (6.5), which is solved using the reduced space successive quadratic programming algorithm (rSQP) provided with the `Moocho` package of the `Trilinos C++` library [15].

In this section we touch only briefly on the numerical implementation of the discrete Dirichlet-to-Neumann map for a collection of spheres, and we refer to [2] for more details on the rSQP technique used for the search of constrained minima.

In principle, standard surface meshing techniques could be employed to integrate on the surface of our swimmer, but they lack the speed and accuracy that specialized methods can offer when integrating on such special domains like collections of spheres.

The method we have chosen for the integration on the spheres is presented in [16] for use with smooth functions and experimental data. It uses an oblique array of integration sampling points based on a chosen pair of successive Fibonacci numbers.

The pattern which is obtained on each sphere has a familiar appearance of intersecting spirals, avoiding the local anisotropy of a conventional latitude-longitude array. We modified the original method to take explicitly into account multiple spheres and the singularity of the Stokeslet (see [28] for a more detailed introduction on boundary integral methods for viscous flow).

The discrete versions \mathbf{u}_h and \mathbf{f}_h of the continuous velocity and force densities \mathbf{u} and \mathbf{f} are obtained by sampling the original functions at the quadrature points, translated and replicated on each sphere according to ξ and p , to obtain N_V scalars that represent $N_V/3$ vectors applied to the quadrature points sampled on $\partial\Omega$.

Integration on $\partial\Omega$ of the function $\mathbf{u}_h(\mathbf{x})$ is then effectively approximated by

$$\int_{\partial\Omega} \mathbf{u}(\mathbf{x}) d\sigma(\mathbf{x}) \sim \sum_{i=1}^{N_V/3} \mathbf{u}(\mathbf{q}^i) \omega^i,$$

where the weights ω^i and quadrature points \mathbf{q}^i are derived according to [16].

The construction of a discrete Dirichlet-to-Neumann map for our swimmers follows the usual collocation method (see, for example, [29]),

$$\begin{aligned} \mathbf{u}(\mathbf{q}^i) &= \int_{\partial\Omega} \mathbf{G}(\mathbf{y} - \mathbf{q}^i) \mathbf{f}(\mathbf{y}) d\sigma(\mathbf{y}) \\ &\sim \sum_{j=1, j \neq i}^{N_V/3} \mathbf{G}(\mathbf{q}^j - \mathbf{q}^i) \mathbf{f}(\mathbf{q}^j) \omega^j + \overline{\mathbf{G}}^{ii} \mathbf{f}(\mathbf{q}^i) \omega^i \quad i = 1, \dots, N_V/3. \end{aligned} \quad (7.1)$$

A specialized calculation of the singular integral is performed in Equation (7.1) when i is equal to j , by deriving $\overline{\mathbf{G}}^{ii}$ according to the (known) exact solution of the flow around a sphere.

Equation (7.1) can be expressed more compactly as:

$$\mathbf{f}_h = \mathcal{A}^{-1} \mathbf{u}_h, \quad (7.2)$$

where the matrix \mathcal{A} is obtained by writing explicitly the various components of Equation (7.1), and we have used the notation \mathbf{u}_h and \mathbf{f}_h to indicate the N_V dimensional vector that samples the functions $\mathbf{u}(\mathbf{x})$ and $\mathbf{f}(\mathbf{x})$ at the quadrature points \mathbf{q} .

The construction of the discrete Dirichlet-to-Neumann map allows us to compute explicitly, given a pair of shape and position variables (ξ, p) , the numerical approximations of $G_h(\xi)$ and $V_h(\xi, p)$. These can in turn be used to solve the constrained minimization problem as in [2], i.e., by using the implementation of the rSQP method included in the Moocho package of the Trilinos library [9].

8. Numerical Results. In this section we analyze some of the optimal strokes that can be obtained with our software for the case of the three-sphere swimmer in the plane [23] (3SP), depicted in Figure 2.2. While this is one of simplest possible extension of the three-sphere swimmer by Najafi and Golestanian [27], it adds already a high degree of complexity to the numerical approximation scheme.

The added complexity comes both from the presence of three additional time dependent variables (one shape and two positions), and from the fact that the vector field that relates positional changes to shape changes ($\dot{p} = \mathbf{V}(\xi, p) \cdot \dot{\xi}$) depends also (though in an explicit way) on the orientation $\theta = p_3$ of the swimmer.

In the software used to compute the optimal strokes for axisymmetric swimmers [2], there is only one position variable $p_1(t) = c(t)$, which can be obtained by post-processing the vector field $\mathbf{V}(\xi)$ (which, in the axisymmetric case, is independent on the position p) and ξ itself.

In the present case of a planar swimmer, this is no longer possible, and the optimization software has to go from optimizing over the *two* shape variables $\xi_1(t)$ and $\xi_2(t)$ to optimizing over the entire shape-position space, composed of the *six* time dependent variables $\xi(t) = (\xi_1(t), \xi_2(t), \xi_3(t))$ and $p(t) = (c_x(t), c_y(t), \theta(t))$.

In the experiments that follow, we use water at room temperature (20° C) as the surrounding fluid, and we express lengths in millimeters (mm), time in seconds (s) and weight in milligrams (mg). Using these units, the viscosity of water is approximately one ($1mPa s = 1mg mm^{-1} s^{-1}$), and the energy is expressed in pico-Joules ($1pJ = 1mg mm^2 s^{-2} = 10^{-12}J$).

The radius of each ball of the swimmer is $.05mm$, and additional constraints are added to the optimization software to ensure that each component of the shape variable ξ stays in the interval $[.1mm, .7mm]$, so that the balls never touch each other and that they don't separate too much.

We present some of the computed optimal strokes that illustrate the richness of the problem. In all the examples that follow, we ask the swimmer to go from $p(0) = (0mm, 0mm, \theta_0)$ to $p(T) = (.01mm, 0mm, \theta_T)$, for various combinations of θ_0 , θ_T and $\xi(0) = \xi(T)$.

Since the swimmer is $2\pi/3$ periodic, it is sufficient to study the optimal strokes varying θ_0 between 0 and $2\pi/3$ while keeping c_x and c_y constant to explore all possible optimal swimming strokes. All other combinations can be obtained by rotations and permutations between the components of the optimal solution (ξ, p) .

Moreover, since rotating the swimmer by π is equivalent to asking it to swim in the opposite direction, reversibility of Stokes flow allows us to further reduce the study of the optimal strokes to the interval $\theta_0 \in [0, \pi/3]$.

In particular, if the pair $\xi(t)$ and $p(t) = (\mathbf{c}(t), \theta(t))$ is an optimal solution of (6.5), then we have that all the following permutations, symmetries and rotations of (ξ, p) are also optimal swimming strokes, but with different initial and final positions:

$$\xi(t) \quad \mathbf{c}(t) + k, \theta(t) \quad \forall k \in \mathbf{R}^2 \quad (8.1a)$$

$$\xi(t) \quad \mathcal{R}_z(\gamma)\mathbf{c}(t), \theta(t) + \gamma \quad \forall \gamma \in [0, 2\pi] \quad (8.1b)$$

$$\xi_2(t), \xi_3(t), \xi_1(t) \quad \mathcal{R}_z(2\pi/3)\mathbf{c}(t), \theta(t) \quad (8.1c)$$

$$\xi_3(t), \xi_1(t), \xi_2(t) \quad \mathcal{R}_z(4\pi/3)\mathbf{c}(t), \theta(t) \quad (8.1d)$$

$$\xi(T-t) \quad \mathbf{c}(T-t) - \mathbf{c}(T), \theta(T-t). \quad (8.1e)$$

Given a family of optimal solutions with different starting angles $\theta_0 \in [0, \pi/3]$, then properties (8.1) can be used to derive the optimal solutions in all of the interval $[0, 2\pi]$.

The optimal strokes we present have been formatted to show the trajectory of the center of the swimmer amplified by a factor 60 with respect to the dimensions of the swimmer itself, and the orientation θ of the swimmer amplified by a factor 10. The full configuration of the swimmer is shown at ten equally spaced times between $t = 0$ and $t = T = 1$.

Our first optimal stroke (Figure 8.1) is obtained by fixing the initial and final rotation $\theta_0 = \theta_T$ to be zero and the initial shape of the swimmer to be $\xi = (.4, .4, .4)mm$. The total energy consumption to swim by $.01mm$ in the x direction with a single stroke is $0.511pJ$.

The first important thing to notice is that, although the initial configuration is symmetric with respect to the translation axis, the stroke is not. This implies that the optimal solution is not unique: exchanging the off axis shape variables $\xi_2(t)$ and $\xi_3(t)$ yields to the same final displacement with the same total energy consumption.

A configuration which is symmetric with respect the y -axis can be obtained by setting $\theta_0 = \pi/6$, and also in this case the solution is non-symmetric and non-unique.

Given the permutation properties (8.1), we deduce that two distinct global solutions with the same energy dissipation exist for $\theta_0 = N\pi/6$, for any integer N . From the existence of these different global minima we can deduce that at least two branches of *local* minima exist outside those particular points, starting off as continuous perturbations of the two global solutions.

Numerical evidence show that at least three stable branches exist, as shown in Figure 8.2, where we plot the energy dissipation of all the (local) optimal strokes with respect to the starting initial angle $p_3(0) = \theta_0$. It is possible to steer the software

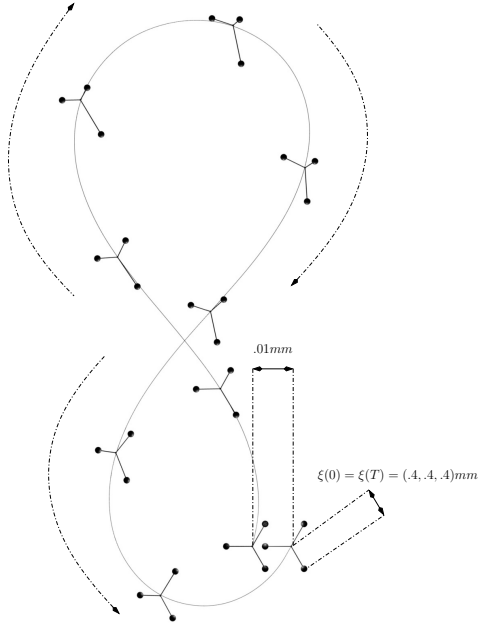


FIG. 8.1. 3SP swimmer: optimal stroke for $\theta_0 = 0 = \theta_T$ radians. The initial shape is fixed at $\xi(0) = \xi(T) = (.4, .4, .4)mm$. Energy consumption to swim by .01mm in the x -direction: 0.511pJ.

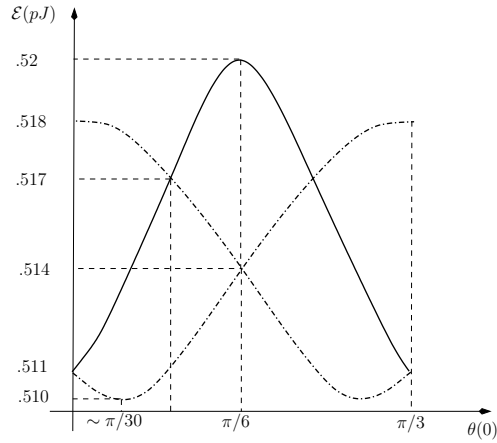


FIG. 8.2. Branches of optimal swimming for 3SP swimmer: dissipated energy VS starting angle.

towards one or the other local branch by feeding it with initial guesses which are close to the desired branch.

From Figure 8.2 it is also clear that the swimmer prefers to swim along directions which are close to parallel to one of the arms: $N\pi/3 \pm \pi/30$ are the approximate preferred swimming directions. The directions perpendicular to one of the arms ($\theta_0 = \pi/6 + N\pi/3$) are the most expensive ones (although they differ in energy only by approximately 2%).

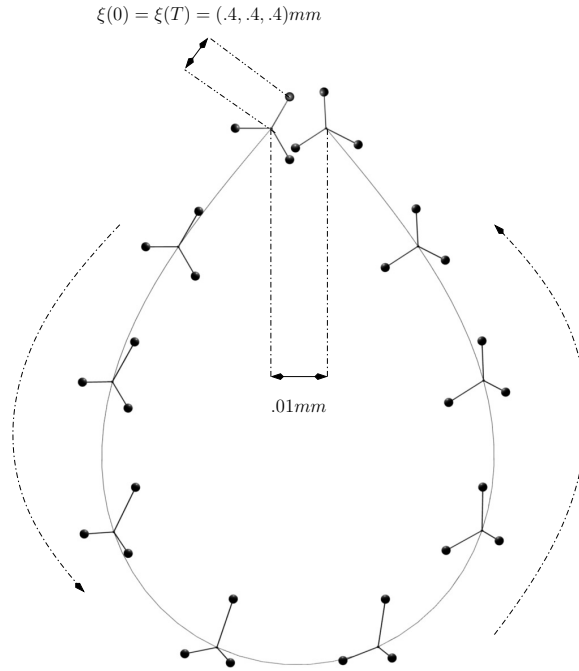


FIG. 8.3. *3SP swimmer: optimal stroke for $\theta_0 = 0$, θ_T optimized to .058 radians. The initial shape is fixed at $\xi(0) = \xi(T) = (.4, .4, .4)mm$. Energy consumption to swim by .01mm in the x -direction: .209pJ.*

From Figure 8.1 it is evident that a lot of energy is wasted in forcing the final rotation to be equal to the initial one. If we relax this requirement and allow the software to optimize the stroke without forcing the rotation to be periodic in time, then the swimmer does not follow an “eight-shaped” path anymore, and the actual target displacement is reached with a smaller stroke (Figure 8.3), and by dissipating less than half the energy (.209pJ instead of .511pJ). The final rotation is approximately .058 radians (about 3.3 degrees).

The main defect associated with this strategy is that all successive strokes will be rotated with respect to the initial swimming direction. If the stroke were to be repeated, we would observe a rotational drift and an average circular motion along a trajectory of radius $r = .35mm$. To ensure that several successive strokes produce an average trajectory along a straight line, one cannot use copies of the same stroke. Instead, different optimization problems need to be solved for each stroke, in each of which the initial orientation is the one reached at the end of the previous stroke.

A complementary strategy to reduce the energy of a single stroke without gener-

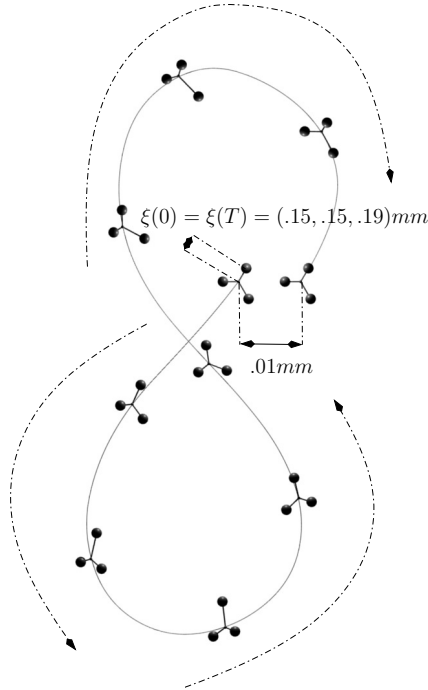


FIG. 8.4. *3SP swimmer: optimal stroke for $\theta_0 = 0 = \theta_T$. The initial shape is optimized to $\xi(0) = \xi(T) = (.15, .15, .19)mm$. Energy consumption to swim by $.01mm$ in the x -direction: $.221pJ$.*

ating a rotated final configuration consists in optimizing also on the starting shape, rather than on the final angle. Figure 8.4 shows this strategy, where the final angle is fixed to be equal to the initial angle. From the figure it is clear that the more complex hydrodynamic interaction due to the closeness of the spheres can be effectively exploited by the optimization software to reduce the dissipated energy.

The optimal initial shape is found to be $(.15, .15, .19)mm$, a non-symmetric shape. The total energy dissipation with this stroke strategy is about $.221pJ$. While this is already less than half of the energy consumed by our first optimal stroke (Figure 8.1), it is still about 10% more expensive than the second attempt (Figure 8.3).

The combination of the two strategies, in which both the initial shape and the final angle are left free for the software to optimize, is shown in Figure 8.5. In this case the total energy dissipation drops down to $.100pJ$. The initial shape is optimized to

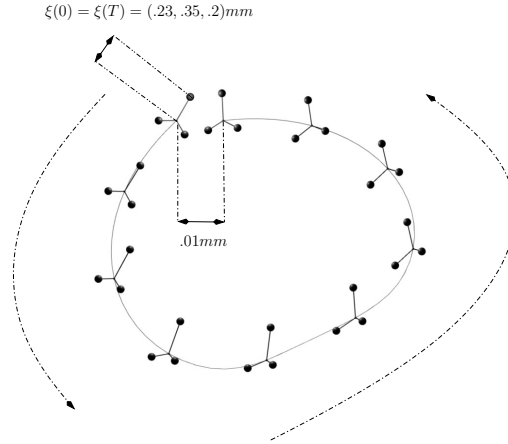


FIG. 8.5. *3SP swimmer: optimal stroke for $\theta_0 = 0$, θ_T optimized to .057 radians. The initial shape is optimized to $\xi(0) = \xi(T) = (.23, .35, .2)mm$. Energy consumption to swim by .01mm in the x -direction: .100pJ.*

the value $(.23, .35, .2)mm$ and the final angle is 0.057 radians, or about 3.28 degrees. In this case the optimal stroke hits the boundary of the region of allowed shapes.

Acknowledgments: The first and last authors benefited from the support of the “Chair Mathematical modelling and numerical simulation, F-EADS – Ecole Polytechnique – INRIA – F-X”

REFERENCES

- [1] A.A. Agrachev and Y.L. Sachkov. *Control theory from the geometric viewpoint*. Springer Heidelberg, 2004.
- [2] F. Alouges, A. DeSimone, and L. Heltai. Numerical strategies for stroke optimization of axisymmetric microswimmers. *Mathematical Models and Methods in Applied Sciences*, 03(21), 2011.
- [3] F. Alouges, A. DeSimone, and A. Lefebvre. Optimal strokes for low Reynolds number swimmers: an example. *J. Nonlinear Sci.*, 18(3):277–302, 2008.
- [4] F. Alouges, A. DeSimone, and A. Lefebvre. Biological Fluid Dynamics, Nonlinear Partial Differential Equations. *Encyclopedia of Complexity and Systems Science*, 2009.
- [5] F. Alouges, A. DeSimone, and A. Lefebvre. Optimal strokes for axisymmetric microswimmers. *The European Physical Journal E*, 28(3):279–284, mar 2009.
- [6] J. E. Avron, O. Gat, and O. Kenneth. Optimal Swimming at Low Reynolds Numbers. *Phys. Rev. Lett.*, 93(18):186001, Oct 2004.
- [7] W. Bangerth, R. Hartmann, and G. Kanschat. *deal.II Differential Equations Analysis Library, Technical Reference*.

- [8] W. Bangerth, R. Hartmann, and G. Kanschat. `deal`. II—a general-purpose object-oriented finite element library. *ACM Trans. Math. Softw.*, 33(4):24, 2007.
- [9] R. A. Bartlett. Mathematical and high level overview of moocho. Technical Report SAND2009-3969, Sandia National Laboratories, 2009.
- [10] A. Bressan. Impulsive control of Lagrangian systems and locomotion in fluids. *Discrete and Continuous Dynamical Systems*, 20(1):1, 2008.
- [11] T. Chambrion and A. Munniert. Generalized Scallop Theorem for Linear Swimmers. *Preprint, arXiv:1008.1098v1 [math-ph]*, 2011.
- [12] G. Dal Maso, A. DeSimone, and M. Morandotti. An Existence and Uniqueness Result for the Motion of Self-Propelled Microswimmers. *SIAM J. Math. Analysis*, 3(43):1345–1368, 2011.
- [13] R. Dreyfus, J. Baudry, and H. A. Stone. Purcell’s “rotator”: mechanical rotation at low Reynolds number. *The European Physical Journal B-Condensed Matter and Complex Systems*, 47(1):161–164, 2005.
- [14] R. et al. Dreyfus. Microscopic artificial swimmer. *Nature*, 7080(437):862–8656, 2005.
- [15] M. A. Heroux et al. An overview of the Trilinos project. *ACM Trans. Math. Softw.*, 31(3):397–423, 2005.
- [16] J. H. Hannay and J. F. Nye. Fibonacci numerical integration on a sphere. *Journal of Physics A: Mathematical and General*, 37:11591–11601, 2004.
- [17] J. Happel and H. Brenner. *Low Reynolds number hydrodynamics with special applications to particulate media*. Prentice-Hall Inc., Englewood Cliffs, N.J., 1965.
- [18] R.M. Harshey. Bacterial motility on a surface: many ways to a common goal. *Annual Reviews in Microbiology*, 57(1):249–273, 2003.
- [19] V. Jurdjevic. *Geometric control theory*. Cambridge Univ Press, 1997.
- [20] A. Y. Khapalov. Local Controllability for a “Swimming” Model. *SIAM Journal on Control and Optimization*, 46:655, 2007.
- [21] J. Koiller, K. Ehlers, and R. Montgomery. Problems and progress in microswimming. *Journal of Nonlinear Science*, 6(6):507–541, 1996.
- [22] E. Lauga and T.R. Powers. The hydrodynamics of swimming microorganisms. *Reports on Progress in Physics*, 72:096601, 2009.
- [23] A. Lefebvre-Lepot and B. Merlet. A stokesian submarine. In *ESAIM: Proceedings*, volume 28, pages 150–161. edpsciences.org, 2009.
- [24] M. J. Lighthill. On the squirming motion of nearly spherical deformable bodies through liquids at very small reynolds numbers. *Comm. on Pure and Applied Math.*, 5(2):109–118, 1952.
- [25] J. Lohéac, J.-F. Scheid Martin, and M. Tucsnak. Controllability by the shape of a low Reynolds number swimmer. *Preprint*, 2011.
- [26] J. San Martín, T. Takahashi, and M. Tucsnak. A control theoretic approach to the swimming of microscopic organisms. *Quart. Appl. Math.*, 65:405–424, 2007.
- [27] A. Najafi and R. Golestanian. Simple swimmer at low Reynolds number: Three linked spheres. *Phys. Rev. E*, 69(6):062901, Jun 2004.
- [28] C. Pozrikidis. *Boundary integral and singularity methods for linearized viscous flow*. Cambridge Texts in Applied Mathematics. Cambridge University Press, Cambridge, 1992.
- [29] C. Pozrikidis. *A practical guide to boundary element methods with the software library BEM-LIB*. Chapman & Hall/CRC, Boca Raton, FL, 2002.
- [30] E.M. Purcell. Life at low Reynolds numbers. *Am. J. Phys.*, 45(1):3–11, 1977.
- [31] A. Shapere and F. Wilczek. Geometry of self-propulsion at low Reynolds number. *Journal of Fluid Mechanics*, 198:557–585, 1989.
- [32] G. Taylor. Analysis of the swimming of microscopic organisms. *Proceedings of the Royal Society of London. Series A, Mathematical and Physical Sciences*, 209(1099):447–461, 1951.